Journal of Zhejiang University-SCIENCE A (Applied Physics & Engineering)
ISSN 1673-565X (Print); ISSN 1862-1775 (Online)
www.zju.edu.cn/jzus; www.springerlink.com
E-mail: jzus@zju.edu.cn

Tool wear criterion, tool life, and surface roughness during high-speed end milling Ti-6Al-4V alloy*

Song ZHANG, Jian-feng LI

(*MOE, Key Laboratory of High Efficiency and Clean Mechanical Manufacture, School of Mechanical Engineering, Shandong University, Jinan 250061, China*)

E-mail: zhangsong@sdu.edu.cn; ljf@sdu.edu.cn

Received Dec. 20, 2009; Revision Mar. 8, 2010; Crosschecked July 19, 2010

Abstract: The objective of the present research is to investigate the relationship among tool wear, surface topography, and surface roughness when high-speed end milling Ti-6Al-4V alloy, and also to define an optimal flank wear criterion for the cutting tool to integrate tool life and the surface roughness requirements of the finish milling process. An annealed Ti-6Al-4V alloy was selected as the workpiece material, undergoing end milling with uncoated carbide inserts. The flank wear of the insert was observed and measured with the toolmaker's microscope. To examine machined surfaces, 3D surface topography was provided by the white light interferometer, and the arithmetical mean roughness (R_a) was calculated with the WYKO Vision32 software. The flank wear increases with cutting time, and the maximal flank wear is set as the flank wear criterion. As the cutting process progresses, tool wear is the predominant factor affecting the variation of surface roughness. According to the plots for the tool wear propagation and surface roughness variation, an optimal flank wear criterion can be defined which integrates the tool life and the surface roughness requirements for the finish milling process.

Key words: Tool wear, Surface topography, Surface roughness, Optimal flank wear criterion
doi:10.1631/jzus.A0900776 **Document code:** A **CLC number:** TG501.1

1 Introduction

Ti-6Al-4V alloy is widely used in many industries owing to the combination of high strength-to-weight ratio, excellent corrosion resistance, fatigue properties, and fracture toughness (Rahman *et al*., 2006; Amin *et al*., 2007). Certain characteristics, however, such as low thermal conductivity, strong chemical reactivity with the cutting tool materials at high temperatures, and relatively low elastic modulus, make it one of the classical difficult-to-cut materials (Ezugwu and Wang, 1997; Corduan *et al*., 2003; Venugopal *et al*., 2007). As a result, the cutting edge rapidly wears (Zoya and Krishnamurthy, 2000), and high wear rate leads to low machining efficiency, poor machining quality, and high production cost. It is essential to approach the most acceptable compromise among high machining efficiency, low production cost, and desired machining quality.

Surface topography, the detailed description of surface characteristics (Toh, 2004), mainly exists in the form of tool marks left by the cutting tool on the machined surface (Mativenga and Hon, 2003). Surface topography can be classified into three categories according to causes, i.e., form error, waviness, and surface roughness (Udupa *et al*., 2000). Surface roughness is an important factor determining functional behaviors of the machined components, i.e., friction, lubrication, wear, sealing, and contact rigidity (Li *et al*., 2000). Surface roughness can be characterized by various parameters; however, the arith-

* Project supported by the National Key Science & Technology Specific projects (No. 2009ZX0400-032), the Taishan Scholar Program Foundation of Shandong Province, the Scientific Research Foundation for Outstanding Young Scientist of Shandong Province (No. 2007BS05001), and the Specialized Research Fund for the Doctoral Program of Higher Education (No. 20070422033), China

metical mean roughness (R_a) is among the most common parameters for surface roughness, and averages all peaks and valleys of the roughness profile, neutralizing the effects of the extreme points in the measurement.

Surface roughness generated in the milling processes is normally related to the height of the remaining materials on the machined surface. For a very sharp cutting tool, the surface roughness of a machined part is principally determined by the cutting conditions, such as cutting speed, feed rate, radial depth of cut, axial depth of cut, tool geometry, cutting configuration, etc. (Jung *et al*., 2005). Sun and Guo (2009) investigated the effects of cutting parameters on surface roughness when end milling Ti-6Al-4V alloy, and indicated that the surface roughness value increased with the feed and the radial depth of cut, while the surface roughness had much less variation with the cutting speed range. Ginting and Nouari (2009) searched the optimal cutting condition for the best surface roughness value when titanium alloy Ti-6242S was end milled with uncoated carbide tools. As the cutting process progresses, however, the cutting edges wear out gradually. The tool wear can change the relative position between the workpiece and the cutting edge, whereby the machined surface is no longer ideal. As a result, surface topography and surface roughness both vary with the tool wear propagation (Oraby and Alaskari, 2008). Knowledge about tool wear variation is beneficial to helping the manufacturers control the cutting process, minimize product cost, and improve machining quality and efficiency. Controlling tool wear magnitude is helpful for improving surface roughness, but it usually increases manufacturing cost. It is very important to achieve the most acceptable compromise between tool wear magnitude and surface roughness requirement to minimize manufacturing costs and improve product quality. Based on the tool wear criterion, integrated surface roughness requirements, and the tool wear, not only can the expected surface roughness be achieved, but also tool life can be prolonged.

The end milling process is designed to remove materials by the relative motion between the cutting tool and the workpiece. The cycloid trajectory of the cutting edge results in that the milled surface topography becoming less uniform than that resulting from the turning operation. The surface roughness along the feed direction is somewhat different from that along the step-over direction (Zhang and Guo, 2009). Especially as the feed rate increases under high-speed machining conditions, the effect of feed rate on surface roughness is no longer negligible (Jung *et al*., 2005). Accordingly, the effect of measuring methods on the surface roughness level is very important in accurately evaluating the surface roughness in the high-speed milling process.

The surface roughness is most commonly measured with a 2D stylus-type profiler meter, which cannot provide 3D information about the surface, and the measurements are time-consuming (Stephenson and Agapiou, 2005). To characterize 3D surfaces, non-contact optical profilometry with white light interferometry has been developed, offering a rapid, reliable, and convenient method of performing 3D surface topography, as well as providing deeper insights into the surface nature through the software capabilities. More important, white light interferometer can calculate the surface roughness over the entire scanning area.

With the popular applications of Ti-6Al-4V alloy in aerospace, medical, power plant, and chemical processing industries, where the machined components must have good dimensional accuracy and surface integrity, it is essential to investigate the tool wear propagation and the surface roughness variation in high-speed milling process. On the other hand, one desires the most acceptable compromise between the tool wear propagation and the surface roughness requirements to reduce manufacturing costs and improve product quality. The present research has the objective of determining the relationship between tool wear, surface topography and surface roughness during the high-speed end milling of Ti-6Al-4V alloy with uncoated carbide inserts. As well, an optimal flank wear criterion is defined, allowing for integration of the tool life and the surface roughness requirements for the finish milling process.

2 Methodology

2.1 Experimental design

2.1.1 Workpiece material

An annealed Ti-6Al-4V alloy was selected as the workpiece material, and its chemical compositions

and material properties at room temperature are provided in Tables 1 and 2, respectively. A rectangular block, 200 mm in length, 114 mm in width and 30 mm in height, was used for the end milling experiments. For the layer-to-layer cutting method was employed in this research, the geometrical configuration of the sample was prepared (Fig. 1).

Table 1 Chemical compositions of Ti-6Al-4V alloy (%, w/w)

Al	V	Fe	Si	C	N	H	O	Titanium
5.60	3.86	0.18	<0.01	0.02	0.023	<0.01	0.17	Balance

Table 2 Material properties of Ti-6Al-4V alloy at room temperature

Density (kg/m^3)	Young's modulus (GPa)	Yield strength (MPa)
4430	113.8	880
Hardness (HB)	**Elongation (%)**	**Reduction in area (%)**
334	14	36

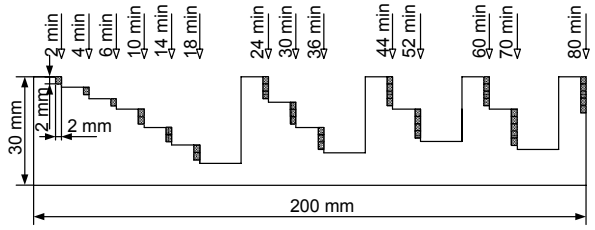

Fig. 1 Geometrical configuration of the sample

2.1.2 Cutting tool and machine tool

A Seco milling cutter with an uncoated carbide insert (Seco grade H25) was used in the end milling experiments. Fig. 2 and Table 3 describe the details of the tooling system. All experiments were conducted on a vertical machining center with a maximal spindle speed of 10000 r/min. A dry cutting environment was used for the milling experiments.

2.2 Experimental procedure

During down milling process, the feed direction of the workpiece was along the negative x-axis; while the step-over direction was along the positive y-axis (Fig. 3). The cutting parameters employed in this research were listed as follows: cutting speed v_c=100 m/min (correspondingly, the spindle speed n was 1273 r/min), feed f_z=0.05 mm/tooth, axial depth of cut a_p=2.0 mm, and radial depth of cut a_e=2.0 mm.

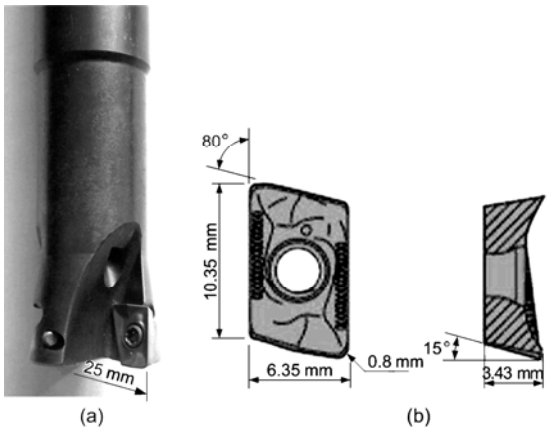

Fig. 2 Geometry of tooling system
(a) Milling cutter; (b) Uncoated carbide insert

Table 3 Details of the tooling system

Item	Description
Toolholder	R217.79
Insert designation	XOMX 090308TR
Cutting tool material	H25
Insert clamping	Collet
Tool diameter (mm)	25
Overhang length (mm)	50
Axial rake angle (°)	+5
Radial rake angle (°)	+5
Clearance angle (°)	−2
Number of insert	1
Corner radius (mm)	0.8
Insert thickness (mm)	3.43
Insert length (mm)	10.35
Insert width (mm)	6.35

To investigate the effects of tool wear propagation on the surface roughness variation, many groups of end milling experiments were conducted. The layer-to-layer cutting method (Fig. 1) was used to mill the Ti-6Al-4V material; that is, when the first layer material was removed, the end miller was controlled to move vertically 2 mm (axial depth of cut a_p) for the next milling process. Layer-to-layer cutting resulted in the previous machined surface being removed by the next milling process, and there was only one milled surface to remain. Accordingly, all the analysis about the surface topography and roughness were limited to one radial depth of cut (2 mm).

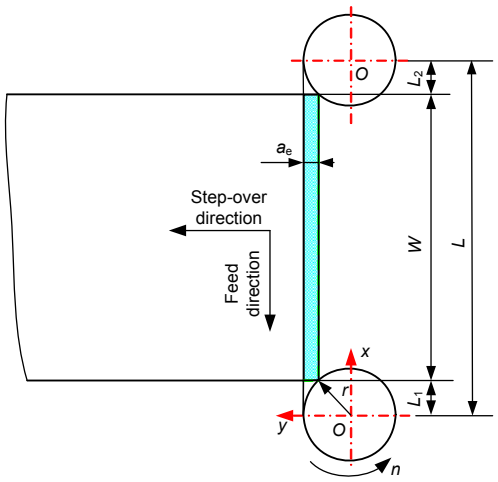

Fig. 3 Schematic diagram of the down milling process

L is the cutting length in one cutting pass (mm), W is the width of the workpiece (mm), L_1 and L_2 are the distances from the tool center to the workpiece edge parallel to x-axis at the starting and ending stages (mm), respectively, r is the radius of the end miller (mm), and n is the rotational speed of the end miller (r/min)

Generally speaking, tool wear increases progressively with cutting time. Therefore, to obtain adequate data about tool wear and surface roughness, the time intervals between two consecutive experiments at the beginning stages were short, while the time intervals at the final stages were relatively long. As shown in Fig. 1, the intervals were 2, 4, 6, 8, and 10 min, respectively. The insert was removed from the tool holder after a given interval, and the flank wear of the insert was observed and measured with the toolmaker's microscope at a 20 times magnification. After the wear observation and measurement, the insert was clamped into the tool holder for the next milling experiment. This procedure was repeated until the tool wear reached the uniform flank wear criterion of 0.3 mm or the maximal wear criterion of 0.5 mm according to (ISO 8688-2, 1989), or by a catastrophic failure. As a result, fourteen milling experiments were conducted, and the total cutting time was 80 min.

The milled samples were degreased by ultrasonic cleaning for 15 min in acetone, and then rinsed with deionized water. The milled surface were observed and measured by a white light interferometer (Veeco NT 9300, USA), which offers a quick, easy, and reliable way to make a non-contact scanning with 0.1 μm vertical resolution. One important advantage of the white light interferometer is that its vertical resolution is independent of the objective's magnification, which allows one to use a low magnification objective to study a large area with a high resolution. During the scanning process, an objective with 2.5 times magnification was selected, and the resolutions along x- and y-axes were both 4 μm. The scanning area at every position was 0.62 mm×1.20 mm, and the vertical scanning speed was set at 2 μm/s. After scanning, the white light interferometer provided the 3D profile of the machined surface and then the arithmetical mean roughness (R_a) was calculated with the WYKO Vision32 software. The average, maximum, and minimum of five R_a results from different scanning areas were used to characterize surface roughness for the milling experiments.

3 Results and discussion

3.1 Cutting time in one cutting pass

As shown in Fig. 3, during down milling process, the end miller starts cutting when the distance from its center to the workpiece edge parallel to x-axis is

$$L_1 = \sqrt{r^2 - (r - a_e)^2}, \tag{1}$$

where r is the radius of the end miller (mm).

Similarly, the milling cutter ends the cutting when the distance from its center to the other workpiece edge parallel to x-axis is L_2, which is equal to L_1.

With the width of the workpiece (W=114 mm), the radius of the milling cutter (r=12.5 mm), and the radial depth of cut (a_e=2.0 mm), the cutting length (L) in one cutting pass is

$$\begin{aligned} L &= L_1 + W + L_2 = W + 2\sqrt{r^2 - (r - a_e)^2} \\ &= 114 + 2\sqrt{12.5^2 - (12.5 - 2.0)^2} = 127.5 \text{ (mm)}. \end{aligned} \tag{2}$$

When the spindle of the machining center rotates at 1273 r/min, the cutting time in one cutting pass (t) is calculated as

$$t = \frac{L / f_z}{n / 60} = \frac{127.5 / 0.05}{1273 / 60} \approx 120 \text{ (s)} = 2 \text{ (min)}. \tag{3}$$

According to Eq. (3), the cutting time in one cutting pass (cutting length is 127.5 mm) is ap-

proximate 2 min. Accordingly, the cutting time can be calculated according to the number of cutting passes.

3.2 Tool wear propagation with cutting time

During high-speed end milling Ti-6Al-4V alloy, the tool wear is much more intense owing to a combination of diffusion and attrition at the cutting zone from the low thermal conductivity and high chemical reactivity of the Ti-6Al-4V alloy. In the analysis of tool wear, the flank wear, which more directly influences the dimensional accuracy and topography of the machined surface, has been commonly emphasized more than the crater wear. The tool life is related to the wear magnitude in different areas of the cutting tool, and the tool life criterion can be set on a certain level of wear. The wear topography on the flank surface of the indexable insert in Fig. 4a indicates that the flank wear is non-uniform. Accordingly, the maximal flank wear, as well as the average flank wear are set as the preferred failure modes of the insert (Fig. 4b). The 0.3-mm average flank wear (VB) and 0.5-mm maximal flank wear (VB_{max}) are adopted in accordance with the standard ISO 8688-2 (1989), and the selection of the tool wear criterion is based on the tool wear propagation to either of these measures of wear, i.e., whichever occurs first.

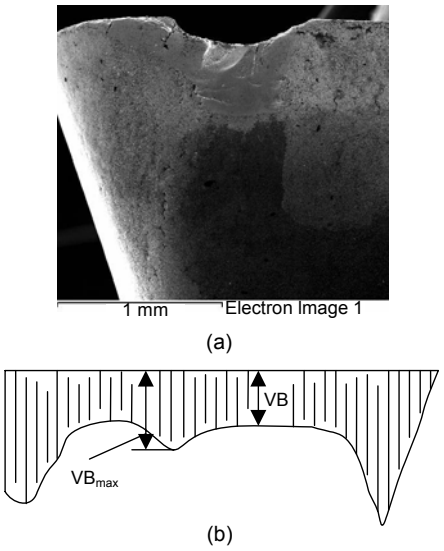

Fig. 4 Flank wear of insert. (a) Flank wear from SEM; (b) Schematic of flank wear area

Fig. 5 shows the variations of the average flank wear and the maximal flank wear with the cutting time. The initial stage (from 0 to 6 min), the so-called, running into wear, is characterized by a high wear rate during a very short period of time. Following the initial wear stage, the cutting tool enters its second phase with nearly a constant wear rate. This stage lasts most of the useful lifetime of the cutting tool until its cutting edge fails, as specified by the standard ISO 8688-2 (1989). The tool life calculation is carried out from the flank wear plots with the cutting time, through interpolation. The tool wear criterion is set at the level where the average flank wear (VB) reaches 0.30 mm or the maximal flank wear (VB_{max}) reaches 0.50 mm, whichever occurs first. Based on the flank wear plots in Fig. 5, the maximal flank wear (VB_{max}= 0.50 mm) first reaches the tool wear criterion specified by the standard ISO 8688-2 (1989) at a cutting time of 63.5 min, though the average flank wear (VB=0.26 mm) is less than 0.30 mm at this point. Accordingly, under these experimental conditions, the maximal flank wear, rather than the average flank wear, is taken as the flank wear criterion.

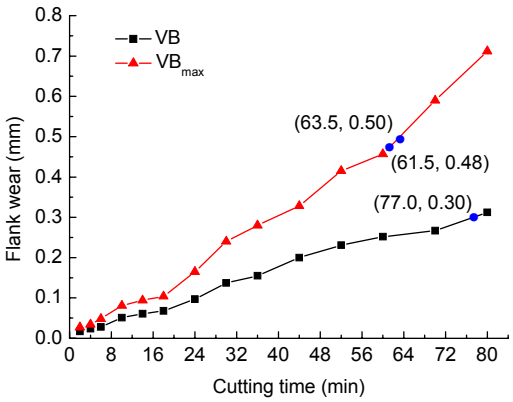

Fig. 5 Flank wear propagation with cutting time

3.3 Surface topography and surface roughness

3.3.1 Surface topography

During the milling process, owing to the combination of the translational motion of the workpiece and the rotational motion of the end miller, the cycloid trajectory of the cutting edge along the feed direction results in the anisotropic distribution of the remaining materials on the machined surface. As a result, the milled surface topography is less uniform than that from the turning process. The 3D machined surface topographies observed by the white light interferometer are shown in Fig. 6, indicating that the distributions of remaining materials along the feed

direction are significantly different from that along the step-over direction. The peaks and valleys of the remaining materials on the machined surface result in the surface irregularities, which form the surface roughness.

3.3.2 Surface roughness

The irregularity of a machined surface consists of high and low regions generated by the cutting edge. These peaks and valleys on the machined surface can be measured and used to evaluate the cutting conditions and the functional performances of the surface. Due to the distribution of the remaining materials, the milled surface is anisotropic. Thus, the surface profile along the feed direction is somewhat different from that along the step-over direction. The surface profiles (after 2 min of milling) along the feed direction (x-axis) and the step-over direction (y-axis) are illustrated in Fig. 7. The maximum peak-valley value along x-axis is 1.36 μm; while the maximum peak-valley value along the y-axis is 2.21 μm. The R_a value along the feed direction is 0.20 μm, which is smaller than that along the step-over direction (0.35 μm). Thus, the measurement direction is one of the important factors influencing the surface roughness level. To reveal the effects of measurement direction on the surface roughness variation, five tracing paths along the feed and step-over directions were randomly selected. The average values derived from five measuring results when the cutting time was 2 min are shown in Fig. 8, which indicates that the surface roughness level is significantly influenced by the measurement direction even when the measurements are conducted on the same milled surface.

In engineering applications, the functional properties of the surface, such as friction, lubrication, wear, sealing, and so forth, are determined by the entire surface. Evaluating the surface roughness from a scanning area rather than from a tracing path is more practical. Thus, to give the surface roughness statistical sense, the 3D surface topographies are measured and R_a values are calculated from at least five scanning areas on the same milled surfaces. The R_a variation with the cutting time is shown in Fig. 9. Similar

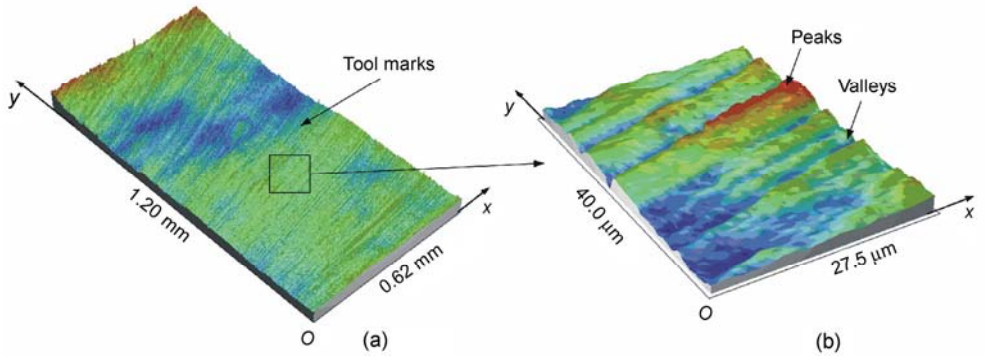

Fig. 6 3D surface topography with white light interferometer. (a) Lower magnification; (b) Higher magnification

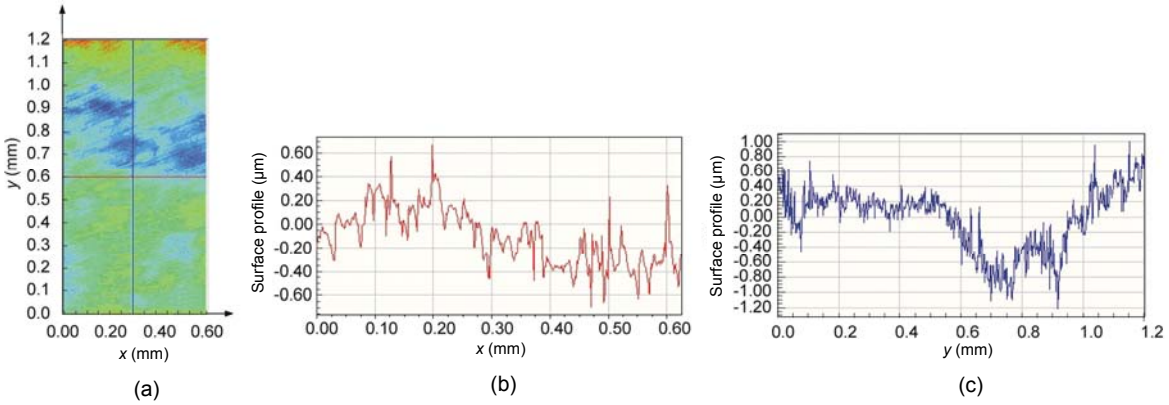

Fig. 7 2D Surface topography and profile (after 2 min of milling). (a) 2D surface topography; (b) Surface profile along x-axis (feed direction); (c) Surface profile along y-axis (step-over direction)

to the relationship between the tool wear propagation and the cutting time, the surface roughness also increases with the increase of the cutting time.

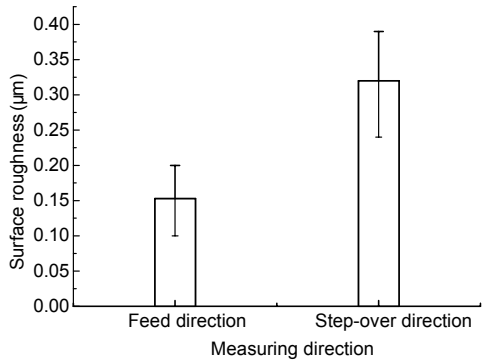

Fig. 8 Surface roughness along different measurement directions (after 2 min of milling)

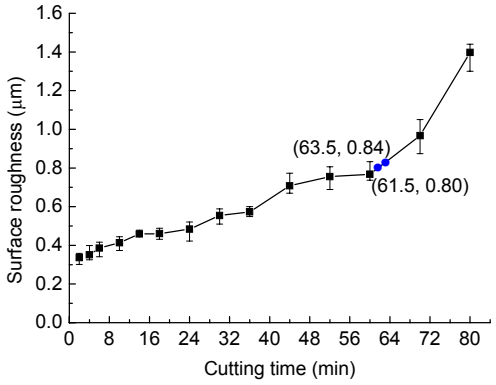

Fig. 9 Surface roughness variation with the cutting time

3.4 Optimal wear criterion integrated tool life and surface roughness

Comparing Fig. 9 with Fig. 5, it can be seen that with an increase in the cutting time, the variation in surface roughness is associated with tool wear propagation. That is to say, the surface roughness increases with the increase of flank wear (VB_{max}). As shown in Fig. 10, the irregularity of a machined surface increases with the increase in tool flank wear. The maximum distance between the lowest valley and the highest peak of the remaining materials on the milled surface induced by the sharp insert (at a cutting time of 2 min, and when the average flank wear is only 0.017 mm) is 4.12 μm. At this point, the surface roughness (R_a) is only 0.34 μm. When the workpiece was milled by a worn insert (with a cutting time of 80 min, and the maximal flank wear reaching 0.71 mm), the maximum distance between the lowest valley and the highest peak of the remaining materials on the milled surface increases to 6.81 μm, and the surface roughness R_a accordingly increases to 1.40 μm.

When the cutting tool is very sharp, the surface topography and roughness are essentially determined by the cutting parameters. This relationship continues until the tool wear begins to progressively develop. At this stage, the surface roughness is significantly influenced by the wear progress to different extents, depending on the wear rate of the cutting edge. Once the wear magnitude reaches beyond a certain value, the deformation of the cutting edge will change the relative position between the cutting tool and the machined materials. As a result, the radial depth of cut and axial depth of cut change with the propagation of the tool wear. The height of the remaining materials on the milled surface accordingly changes. There is no doubt that tool wear is the predominant factor affecting surface topography and surface roughness when the tool wear reaches a certain magnitude.

Surface roughness is often a good item for assessing the functional performances of machined components and the machinability of a particular material. In engineering practices, surface roughness is usually expensive to control during the cutting process. Generally speaking, decreasing surface roughness will shorten tool life and increase machining costs, while improvement in tool life is essential to reduce production costs as much as possible. This often results in a compromise between the machining cost of a component and its surface roughness requirement.

In terms of surface roughness, the tool wear criterion used in this work is that the machined surfaces roughness (R_a) for the finish milling process must be smaller than 0.80 μm to consider the tool to be still operative. Thus, tool life is the total cutting time before the measured surface roughness reaches the critical value R_a=0.80 μm. As mentioned above, the maximal flank wear criterion, VB_{max}=0.5 mm, is selected as the tool wear criterion under the present experimental conditions. The plots of the tool wear propagation and surface roughness variation in Figs. 5 and 9, however, indicate that when the maximal flank wear is 0.5 mm, the surface roughness has increased up to 0.85 μm, which is larger than the limited R_a value (0.80 μm) for the finish milling process.

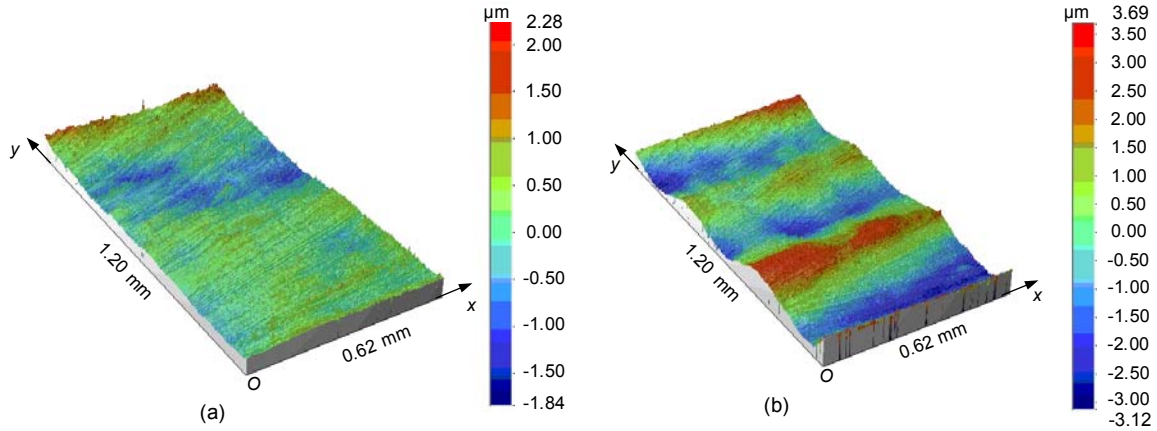

Fig. 10 Surface topography with different flank wear areas (a) after 2 min of cutting time and (b) after 80 min of cutting time

Therefore, to avoid the effect of catastrophic tool wear on surface roughness, it is recommended to cease using the cutting tools before it reaches this condition and to select the proper tool wear criterion based on the surface roughness requirement ($R_a \leq$ 0.80 μm). Accordingly, the maximal flank wear criterion, VB_{max}, is 0.48 mm for the finish milling process, and the corresponding tool life is about 61.5 min. Comparing this with the maximal flank wear criterion VB_{max}=0.50 mm (where the cutting time is 63.5 min), 2 min of tool life are lost, but the integrity of the cutting edges, and especially an expected surface roughness, are ensured. Thus, according to the tool wear curve (Fig. 5) and surface roughness variation curve (Fig. 9), an optimal flank wear criterion, VB_{max}=0.48 mm, can be defined which integrates the tool life and the surface roughness requirements for the finish milling process.

4 Conclusions

This study investigates the tool wear, the surface topography and roughness during high-speed end milling of Ti-6Al-4V alloy with uncoated carbide inserts under dry cutting conditions, and provides the optimal criterion for tool wear integrating the tool life and the surface roughness requirements for the finish milling process. The following conclusions can be drawn:

1. Flank wear increases with cutting time, and the maximal flank wear rather than the average flank wear is set as the flank wear criterion.

2. The cycloid trajectory of the cutting edge in the milling process results in an anisotropic surface topography and roughness. Therefore, it is more practical to evaluate the surface roughness from a scanning area rather than from a tracing path.

3. Surface roughness increases with tool wear, and tool wear is the predominant factor affecting the variations of surface topography and roughness.

4. According to the plots for the tool wear propagation and surface roughness variation, an optimal flank wear criterion can be defined which integrates the tool life and the surface roughness requirements for the finish milling process.

References

Amin, A.K.M.N., Ismail, A.F., Khairusshima, M.K.N., 2007. Effectiveness of uncoated WC-Co and PCD inserts in end milling of titanium alloy—Ti-6Al-4V. *Journal of Materials of Processing Technology*, **192-193**:147-158. [doi:10.1016/j.jmatprotec.2007.04.095]

Corduan, N., Hirnbert, T., Poulachon, G., Dessoly, M., Lambertin, M., Vigneau, J., Payoux, B., 2003. Wear mechanisms of new tool materials for Ti-6Al-4V high performance machining. *CIRP Annals-Manufacturing Technology*, **52**(1):73-76. [doi:10.1016/S0007-8506(07)60534-4]

Ezugwu, E.O., Wang, Z.M., 1997. Titanium alloy and their machinability—a review. *Journal of Materials of Processing Technology*, **68**(3):262-274. [doi:10.1016/S0924-0136(96)00030-1]

Ginting, A., Nouari, M., 2009. Surface integrity of dry machined titanium alloys. *International Journal of Machine Tools and Manufacture*, **49**(3-4):325-332. [doi:10.1016/j.ijmachtools.2008.10.011]

ISO 8688-2, 1989. Tool Life Testing in Milling—Part 2: End-milling. International Organization for Standardization, Geneva, Switzerland.

Jung, T.S., Yang, M.Y., Lee, K.J., 2005. A new approach to analysing machined surfaces by ball-end milling, part I: Formulation of characteristic lines of cut remainder. *International Journal of Advanced Manufacturing Technology*, **25**(9-10):833-840. [doi:10.1007/s00170-003-1930-5]

Li, C.G., Dong, S., Zhang, G.X., 2000. Evaluation of the anisotropy of machined 3D surface topography. *Wear*, **237**(2):211-216. [doi:10.1016/S0043-1648(99)00327-0]

Mativenga, P.T., Hon, K.K.B., 2003. A study of cutting forces and surface finish in high-speed machining of AISI H13 tool steel using carbide tools with TiAlN based coatings. *Proceedings of the Institution of Mechanical Engineers, Part B: Journal of Engineering Manufacture*, **217**(2):143-151. [doi:10.1243/095440503321148786]

Oraby, S.E., Alaskari, A.M., 2008. Surface topography assessment techniques based on an in-process monitoring approach of tool wear and cutting force signature. *Journal of the Brazilian Society of Mechanical Sciences and Engineering*, **15**:221-230. [doi:10.1590/S1678-58782008000300007]

Rahman, M., Wang, Z.G., Wong, Y.S., 2006. A review on high-speed machining of titanium alloys. *JSME International Journal, Series C*, **49**(1):11-20. [doi:10.1299/jsmec.49.11]

Stephenson, D.A., Agapiou, J.S., 2005. Metal Cutting Theory and Practice (2nd Ed.). Taylor & Francis, New York, USA, p.552-557.

Sun, J., Guo, Y.B., 2009. A comprehensive experimental study on surface integrity by end milling Ti-6Al-4V. *Journal of Materials Processing Technology*, **209**(8):4036-4042. [doi:10.1016/j.jmatprotec.2008.09.022]

Toh, C.K., 2004. Surface topography analysis in high speed finish milling inclined hardened steel. *Precision Engineering*, **28**(4):386-389. [doi:10.1016/j.precisioneng.2004.01.001]

Udupa, G., Singaperumal, M., Sirohi, R.S., Kothiyal, M.P., 2000. Characterization of surface topography by confocal microscopy, part I: Principles and the measurement system. *Measurement Science and Technology*, **11**(3):305-314. [doi:10.1088/0957-0233/11/3/320]

Venugopal, K.A., Paul, S., Chattopadhyay, A.B., 2007. Growth of tool wear in turning of Ti-6Al-4V alloy under cryogenic cooling. *Wear*, **262**(9-10):1071-1078. [doi:10.1016/j.wear.2006.11.010]

Zhang, S., Guo, Y.B., 2009. Taguchi method based process space for optimal surface topography by finish hard milling. *ASME, Journal of Manufacturing Science and Engineering*, **131**(5):051003. [doi:10.1115/1.3207740]

Zoya, Z.A., Krishnamurthy, R., 2000. The performance of CBN tools in the machining of titanium alloys. *Journal of Materials of Processing Technology*, **100**(1-3):80-86. [doi:10.1016/S0924-0136]

2009 JCR of Thomson Reuters for *JZUS-A*

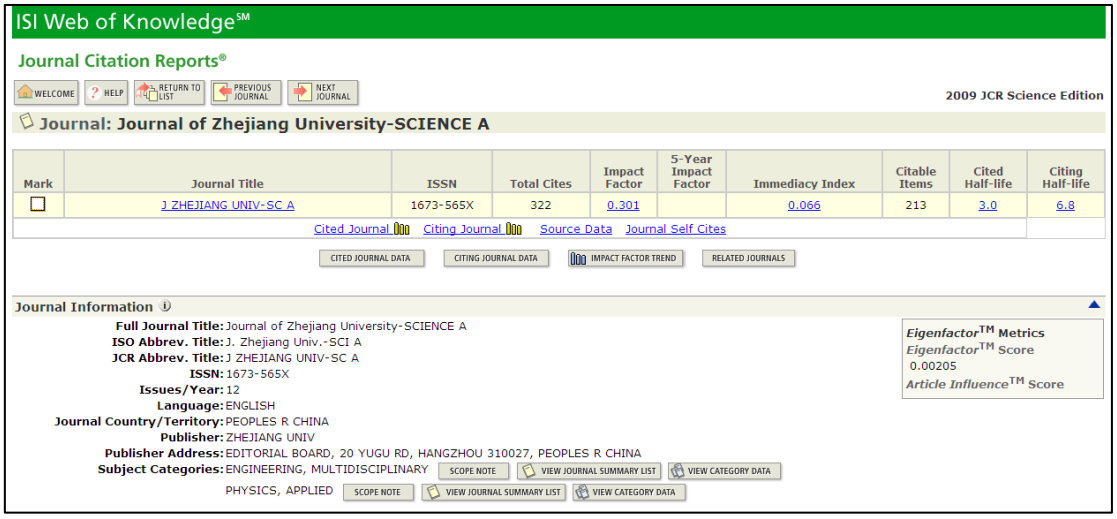
ISI Web of Knowledge℠

Journal Citation Reports®

WELCOME | HELP | RETURN TO LIST | PREVIOUS JOURNAL | NEXT JOURNAL

2009 JCR Science Edition

Journal: Journal of Zhejiang University-SCIENCE A

Mark	Journal Title	ISSN	Total Cites	Impact Factor	5-Year Impact Factor	Immediacy Index	Citable Items	Cited Half-life	Citing Half-life
☐	J ZHEJIANG UNIV-SC A	1673-565X	322	0.301		0.066	213	3.0	6.8

Cited Journal | Citing Journal | Source Data | Journal Self Cites

CITED JOURNAL DATA | CITING JOURNAL DATA | IMPACT FACTOR TREND | RELATED JOURNALS

Journal Information

Full Journal Title: Journal of Zhejiang University-SCIENCE A
ISO Abbrev. Title: J. Zhejiang Univ.-SCI A
JCR Abbrev. Title: J ZHEJIANG UNIV-SC A
ISSN: 1673-565X
Issues/Year: 12
Language: ENGLISH
Journal Country/Territory: PEOPLES R CHINA
Publisher: ZHEJIANG UNIV
Publisher Address: EDITORIAL BOARD, 20 YUGU RD, HANGZHOU 310027, PEOPLES R CHINA
Subject Categories: ENGINEERING, MULTIDISCIPLINARY SCOPE NOTE | VIEW JOURNAL SUMMARY LIST | VIEW CATEGORY DATA
PHYSICS, APPLIED SCOPE NOTE | VIEW JOURNAL SUMMARY LIST | VIEW CATEGORY DATA

Eigenfactor™ Metrics
Eigenfactor™ Score
0.00205
Article Influence™ Score